

Influence of dynamic mechanical stress on lithium-ion-battery aging

CoFAT 2017

F. Ebert*, G. Sextl

Fraunhofer-Institute for Silicate Research ISC
Würzburg, Germany
fabian.ebert@isc.fraunhofer.de

M. Lienkamp

Institute of Automotive Technology
Technical University of Munich
Garching, Germany

Abstract—this paper presents the investigation results of the effects on battery cell aging from onetime crash acceleration loads. In official safety tests, like the UN38.3 or UNECE R100 test aging behavior after the test is not investigated. To investigate possible negative effects after crash loads, two types of battery cells were tested with three different types of crash acceleration loads from real crash data. To observe the effects from mounting orientation, both axial and radial loads were applied. Effects on instant capacity loss after the incident and the overall aging behavior could be observed. Non-destructive computer tomography showed internal damage of the cell that could not be detected externally.

Keywords—lithium-ion-batteries, aging, mechanical stress, internal damage

I. INTRODUCTION

Battery cells are exposed to numerous mechanical stress events in mobile applications. This can be the drop of a cellphone on the floor or, in the case of an electric car, a crash with an obstacle or another car. In addition, periodic mechanical stresses (i.e. vibrations) can occur during operation - e.g. from rough streets [1].

To guarantee customer safety, battery cell manufacturers are obliged to document the robustness of their product via mandatory safety tests. These tests reproduce events that can happen during transport [2] or at accident events [3]. Table 1 shows the shock parameters of the UN38.3.4 transport test for cell and pack level. These tests are characterized by high acceleration but short duration shocks.

Table 1: UN38.3.4 shock test criteria [2]

	UN 38.3.4 shock test	
	Cell level	Pack level
Maximum acceleration	150 g	50 g
Shock duration	6 ms	11 ms
Shock curve	half-sine	half-sine

Acceptance criteria are no leakage or venting of the cell. Additionally, the measured cell voltage must not be less than 90 % of the initial cell voltage.

Acceleration forces of crash events (car to car or car to obstacle) differ significantly in maximum acceleration force and duration. The UN ECE shock curves are characterized by decent maximum acceleration but comparably long shock durations. Table 2 shows the compulsory shock curve data of the UN ECE R100 regulations.

Table 2: UN ECE R100 shock test criteria [3]

Time (ms)	UN ECE R100 shock test (Maximum curve longitudinal)		
	M1/N1 vehicles	M2/N2 vehicles	M3/N3 vehicles
0	10 g	5 g	4 g
50	28 g	17 g	12 g
80	28 g	17 g	12 g
120	0 g	0 g	12 g

Pass criteria are no leakage/venting (or worse) of a cell. Voltage examination is not required.

If compared with the data obtained from real crash events shown in Figure 1, one can clearly see some amount of discrepancy between the official test procedures and the measured data. Acceleration data was measured by sensors placed near the battery pack and therefore represents forces acting on the cells. Matched against test procedure requirements, only the decent AZT front crash with 20 km/h is comparable. More severe crash events like the NCAP front and side crashes are not covered.

If carefully studied, the official safety test procedures do not require the investigation of the battery lifetime or, respectively aging behavior after the shock events. In our opinion, this aspect should be considered for the following reasons:

- Battery packs are designed mechanically robust. Furthermore, the cells are located outside of regions that are deformed at a crash event. Due to this, it is possible that even after a severe crash like during NCAP tests, the battery pack itself shows no external detectable damage signs. Hence, it is conceivable, that these packs are fraudulently sold as accident free on the second-life market as spare parts or for stationary storage.

- After a small or medium crash, it is important for car insurances purposes if the battery loses usable capacity. As this represents a loss of value, the effects of such crashes must be known qualitatively and quantitatively, if possible. Total replacement of the battery pack based just on speculation is financially intolerable for car insurance companies.
- Test data [4] also showed the external undetectable damaging of cell-internal safety devices due to dynamic mechanical stresses. In this investigation, the mandrel was loosened via vibration and damaged the current-interrupt-device CID in an 18650 cell.

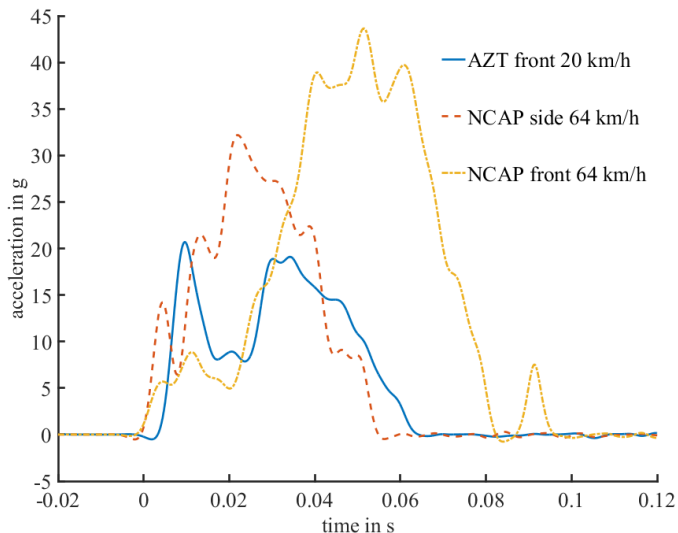


Fig. 1. Crash profile of a AZT front crash of a VW e-Up and NCAP crash test profiles of the TU Munich Visio.m prototype car

II. EXPERIMENT

A. Battery cells

To be able to get information about the influence of battery format, two different cell-types, one cylindrical 18650-type and one prismatic pouch-type, were used. Detailed specifications of the cells are shown in Table 3.

Table 3: Cell type overview

Cell type	Panasonic NCR18650PF	Kokam SLPB396495H
Capacity	2750 mAh	2000 mAh
Nominal Voltage	3.6 V	3.7 V
Dimensions	18 x 65 mm	95 x 64 x 3.9 mm
Weight	48 g	46 g
Nominal charging rate	0.5 C	1 C
Maximum discharge rate	2 C	5 C

B. Conduction of the crash tests

Three test specimens of each cell type were mounted in a fixture shown in Figure 2 with the main axes perpendicular to the direction of crash acceleration (left half of the fixture). Additionally, three test specimens of each cell type were mounted parallel (right half of the fixture) to the direction of crash acceleration in order to guarantee identical crash profiles for each cell orientation. In the case of the pouch-type cells, these were braced with a plate to ensure mechanical stiffness and proper force application. For electrical safety purposes, the whole cell bracket is made of polyoxymethylene (POM).

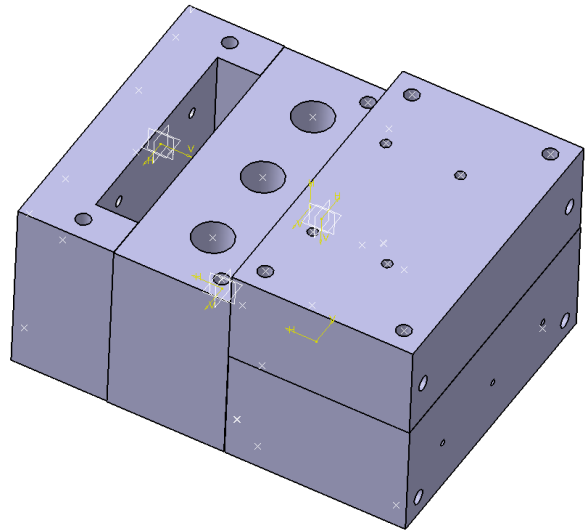


Fig. 2. Cell fixture for crash tests made of polyoxymethylene (POM) for electrical insulation and mechanical robustness.

Due to the long crash pulse durations a crash test accelerator system with sufficient stroke length is needed. Therefore, the tests were conducted on a servo-hydraulic accelerator sled system (Messring Systembau, CIS system). With the help of the active servo-hydraulic accelerator system, custom crash profiles are possible without the need to manufacture special designed crash pads.

C. Cell preparation and post-test cyclization

To identify cell failures prior to the crash test each cell was characterized with five full cycles (CCCV charge to 4.2 V with 0.5 C, cutoff at C/10; CC discharge to 2.5 V (Panasonic) / 3.0 V (Kokam) with 0.5 C). The crash test was performed at 100 % SOC.

After the crash test, the cells were aged with the same CCCV/CV cycle until 80 % SOH. To accelerate aging, cyclization was performed in a climate chamber at 45 °C. For reference, three pristine cells of each type were cyclized as well.

III. FINDINGS

A. Post-crash test observation

Directly after the crash test, the cells were observed for five minutes due to safety reasons. No signs of severe damage, such as leaking or smoking could be observed.

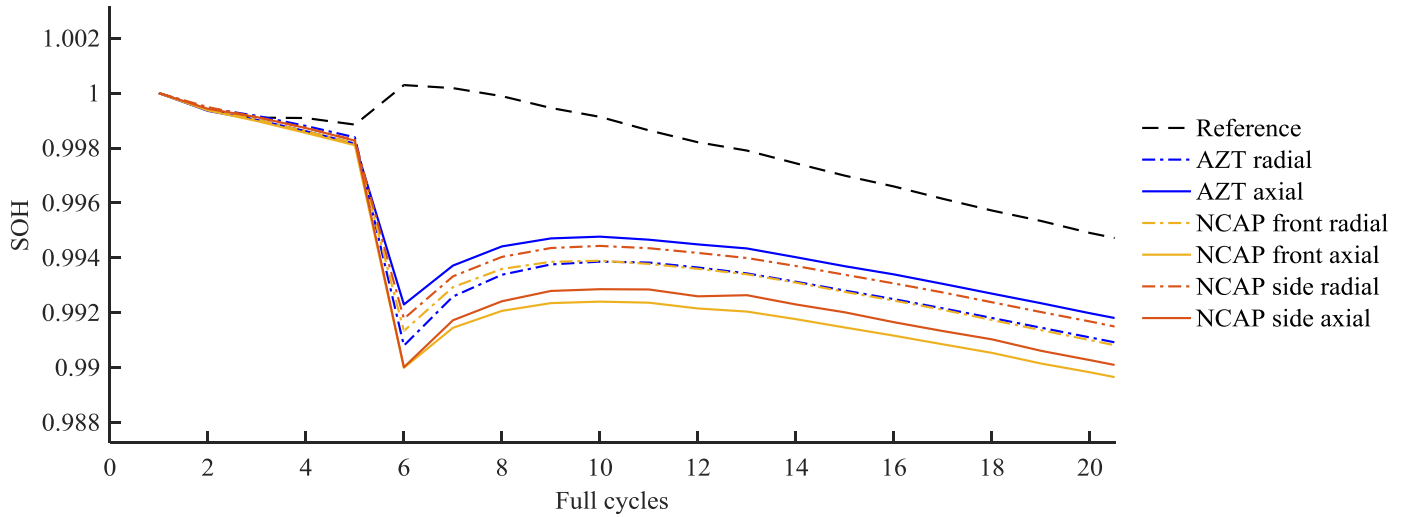


Fig. 3. Initial mean capacity drop and recovery after crash test of 18650 cells

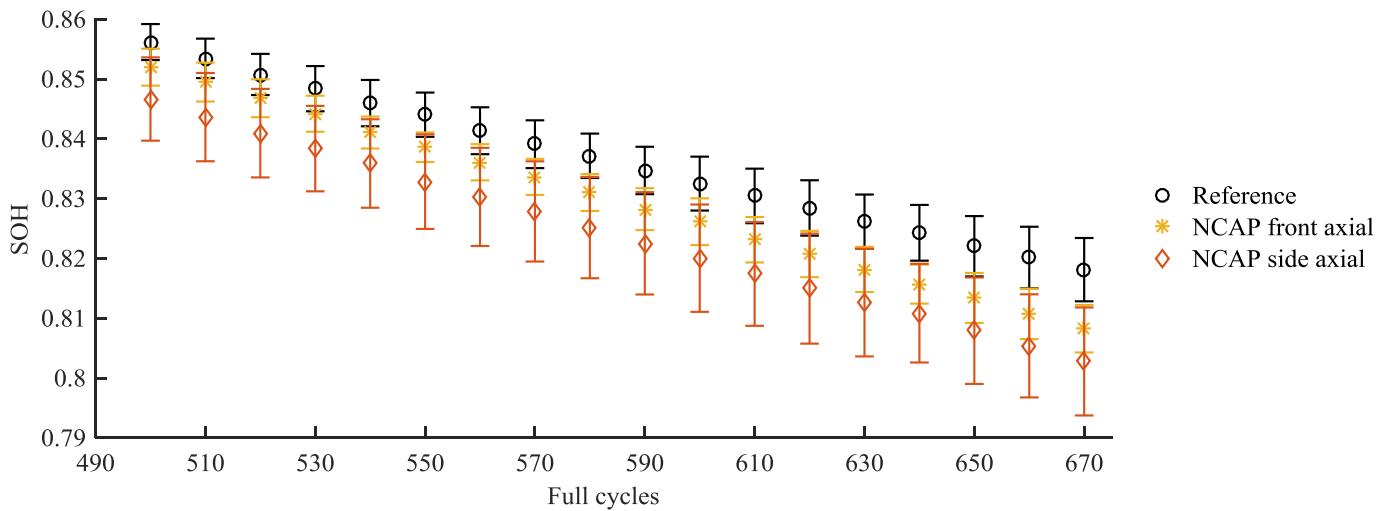


Fig. 4. Aging deviation of 18650 cells after 670 cycles from different crash profiles

A check of the terminal voltage of the cells also showed no noticeable voltage drop. The pouch-type cells also showed no signs of swelling, which can be an indicator of an internal short circuit. In addition, no abnormal warming was detected. With the UN38.3 or UN ECE R100 test procedures, the cells would have passed the test.

B. Aging behavior

For the purpose of comparability and in order to equalize manufacturing variances, the cell capacity was normalized to the capacity of the first measured cycle (= 100 % SOH). Furthermore, the mean and standard deviation of each batch of test samples was calculated to minimize any falsifying effects of outliers. Inspection of the aging data showed three effects:

1. *Immediate drop of cell capacity after the shock test:* Figure 3 shows the cell capacity of the initial five cycles of the 18650 cells before and the

following cycles after the crash test. Each shock-tested cell batch shows a collapse of measured capacity independent of the shock orientation. Furthermore, the capacity decline scales with the maximum at first glance. The un-shocked reference cells show no sign of capacity decline. The increasing capacity is due to the fact that the cells were cycled at 45 °C to accelerate aging, whereas the first five characterizing cycles were conducted at the standard 25 °C. If this effect is also taken into account, the actual capacity drop is even higher.

2. *Partial restoration of capacity:*

One can observe that the cells show some kind of self-healing behavior for the next five to ten cycles after the crash test. In the authors' opinion this is due to restoration of conductive paths that were broken by the crash impact. In connection with the

swelling of the electrode particles from cycling, un-attached electrode particles can be reattached to the rest of the electrode.

3. Deviation of overall aging behavior:

Data from the pouch type cells is not shown here because the applied C-rates showed only a negligible small aging rate even after almost 700 full cycles. This is because the pouch type cells are designed for a nominal discharge rate of 5 C. Due to the small load, no differentiable aging deviation behavior could be observed. In addition, the aging data of the perpendicular orientated cells, as well as the AZT samples, showed no noticeable deviant aging rate compared to the unstressed reference cells. On the contrary, measurably faster aging was observed for the cells shocked with front and side NCAP crash profiles in the axial direction.

As shown in Figure 4, there is a measurable mean difference in the cell capacity after 675 full cycles.

C. Post-mortem analysis

After completion of the cycling tests, one cell of the reference cells, the NCAP side crash and the NCAP front crash cell-batch were chosen for post-mortem analysis. First, a non-destructive analysis via computer tomography was conducted. Figure 5 shows the results of the radiography. A noticeable bending of the electrodes near the collar of the cell casing can be observed in Figure 5a). This is a hint for a translational movement of the jellyroll in the cell casing due to the axial acceleration force of the crash impulse. Electrode bending in the reference cell in Figure 5b) could not be detected. In top-view in Figure 5c) and d) a spatial non-uniform bending of the electrodes can be seen. One can observe that the electrode damage results from contact between the jellyroll and the plastic spacer.

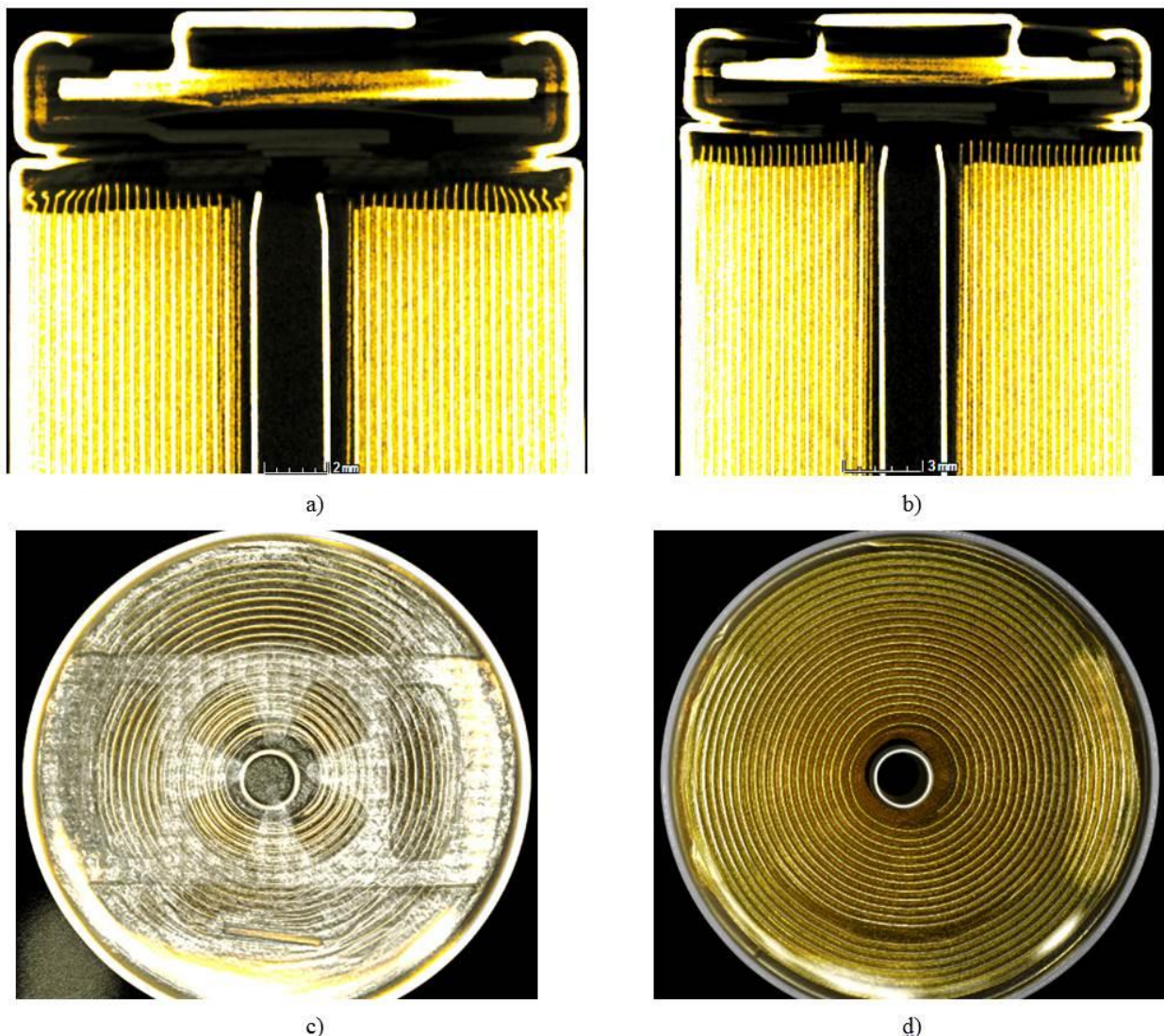


Fig. 5. Tomographies of a cell with a) NCAP side crash profile and b) an unstressed reference cell. One can observe the bent electrodes near the collar of the cell casing, which is an indication of the translational movement of the jellyroll. Top-view pictures show a non-uniform bending of the electrodes due to the spacer shown in c) and d).

If the jellyroll moves in the cell casing as a result of the external acceleration force from a crash the spacer also moves. After a short distance, the spacer is not able to move any further because of the casing collar. Due to the resistance of the collar and the kinetic energy of the jellyroll, the protruding electrode layers are bent until the jellyroll movement stops.

IV. DISCUSSION OF INFLUENCE FACTORS

A. Influence of cell orientation at crash event

The tested 18650 cell-type shows some intrinsic susceptibility to damage from crash acceleration because of its internal structure. The active part of the cell, the jellyroll is fitted relatively loosely in the cell casing compared to e.g. pouch-cell types, where higher mechanical stability is achieved via the cell-internal vacuum and external bracing structures. In 18650-type cells, direct mechanical connection to the cell casing only exists via the two current collectors, which are not very rigid. Due to this fact, the jellyroll is prone to longitudinal displacement if acceleration forces occur in the main axis direction like in the presented experiment.

For that reason, it is not recommended to mount this type of 18650 cells oriented with their main axis in front or side crash direction to prevent jellyroll migration in the cell, even if the measured aging loss is not severe. On the other hand, if cells are mounted with their main axis perpendicular to the road they are exposed to vibrational stress from e.g. road irregularities. This mechanical stress can also lead to non-visible internal cell damage [4].

B. Influence of internal cell structure

In addition, the internal cell structure can have notable influence on the behavior of cells during crash acceleration events. One main factor is the friction between the jellyroll and the cell casing. In this paper, the contact is copper foil (electrode) with aluminum (casing). In other 18650-type cell models, it could be seen that the jellyroll was covered in a layer of separator material, which leads to a different friction coefficient and will therefore show diverging crash movement behavior.

Furthermore, the shape of the plastic spacer on top of the jellyroll can have an impact on the amount of electrode buckling resulting from translational movement of the jellyroll and collision with the spacer. In our case, the non-all-over shape of the spacer leads to local compression force on the jellyroll. For comparison, Figure 6 shows a spacer obtained from a 20700 Samsung cell that has a more all-over shape. In this cell-type, the crash load will be distributed over a larger contact area and electrode buckling will be reduced or even avoided.

If cylindrical cells increase in size like the new cylindrical 21700 format, the jellyrolls gets heavier whereas the surface of the jellyroll does not increase at the same amount. Hence, a heavier jellyroll will tend to migrate in the cell casing earlier. Large format cells, like the prismatic PHEV or BEV cell-types, are connected more robustly with the current collectors and

should not be as prone to acceleration forces like the cylindrical types.



Fig. 6. Nearly all-over cell spacer from a cylindrical Samsung 20700 cell type

C. Influence of cell SOC and SOH

As one of the main factors for translational movement of the jellyroll, the friction coefficient depends on the normal force of the sliding solid to the surface. Therefore, the state-of-charge (SOC) and the state-of-health (SOH) also has influence. If a cell is charged, both the anode material, graphite, and common cathode materials, like nickel-manganese-cobalt oxide (NMC), expand/contract in full, charged/discharged state [5], [6]. In the case of the graphite this can be in the magnitude of around 10 % of the electrode thickness [7]. If silicon-rich anode materials are used, this effect increases even more because silicon shows an overall expansion from an uncharged to charged state of around 300 % [8]. Expansion also occurs from cell aging because of the increasing layer thickness of the solid-electrolyte interface that leads to an increasing overall thickness of the jellyroll [9].

D. Influence of shock profile

In addition, the shock profile will have an influence on the effect on the cells: First, the maximum acceleration and the duration of the shock, which accounts for the overall transmitted energy on the cell, and second, the shape of the crash impulse. Normal test procedures demand half-sine shape pulses. From the acceleration data in Figure 1, it can be seen that real crash profiles differ heavily from half-sine shapes. In the case of the front-crash, two peaks can be observed that result from the contact with the bumper and inner structural elements. For this reason, the possible effect of resonances should be discussed.

V. CONCLUSION AND OUTLOOK

In 18650 cells, onetime axial loads can lead to a translational movement of the jellyroll in the cell casing that is not instantaneously detectable externally e.g. from voltage readings. In this paper, both an instantaneous drop in capacity and an overall diverging aging behavior was observed on new and fully-charged cells. Because mechanical cell properties change from both cell state-of-charge and state-of-health and can vary from model to model, the results cannot be applied to any arbitrary cell type.

Overall, the 18650 cell-type showed a very robust behavior, even in heavy accident test cases like the NCAP crash test profiles. An instantaneous severe safety risk from the shocked cells was not induced and the cells can be labeled as safe after the crash test. Furthermore, no safety relevant operation behavior was observed during the cyclization process in the laboratory. Therefore, second life use of such cells would be possible.

As the capacity loss is negligible for the AZT crash profiles and is in the order of 2 to 3 % for onetime heavy crash NCAP loads it could be discussed to be also negligible. Considering the overall designed mileage of 180.000 km for an electric car the mileage loss from the shock would be approximately 4000 km. Nevertheless, especially the effect from different SOC and SOH will show diverging effects due to altered friction of the jellyroll that could possibly lead to safety relevant effects e.g. internal short circuit or damage of cell internal safety features like the CID as shown in [4].

The mechanisms of the instantaneous loss and partial restoration of usable cell capacity needs further investigation. In addition, effects from the cell format or, respectively, the jellyroll weight as well as the crash acceleration profile will be investigated in the future.

CONTRIBUTIONS

F.E. performed the crash and aging tests of the batteries as well as the interpretation of the tomography and aging data. M.L. made an essential contribution to the conception of the research project. M.L. and G.S. revised the paper critically for important intellectual content. Mr. L. and Mr. S. gave final approval of the version to be published and agrees to all aspects of the work. As a guarantor, M.L. accepts responsibility for the overall integrity of the paper.

REFERENCES

- [1] G. Kjell and J. F. Lang, "Comparing different vibration tests proposed for li-ion batteries with vibration measurement in an electric vehicle," in 2013 World Electric Vehicle Symposium and Exhibition (EVS27), 2013, pp. 1–11.
- [2] United Nations, "Transport of Dangerous goods," *Man. tests criteria*, vol. 5, no. 38, pp. 43–51, 2009.
- [3] United Nations, "UN ECE R100," *World Forum Harmon. Veh. Regul.*, vol. 2, no. 99, pp. 1–82, 2013.
- [4] M. J. Brand, S. F. Schuster, T. Bach, E. Fleder, M. Stelz, S. Gläser, J. Müller, G. Sextl, and A. Jossen, "Effects of vibrations and shocks on lithium-ion cells," *J. Power Sources*, vol. 288, pp. 62–69, 2015.
- [5] N. Zhang and H. Tang, "Dissecting anode swelling in commercial lithium-ion batteries," *J. Power Sources*, vol. 218, pp. 52–55, 2012.
- [6] M. Bauer, M. Wachtler, H. Stöwe, J. V. Persson, and M. A. Danzer, "Understanding the dilation and dilation relaxation behavior of graphite-based lithium-ion cells," *J. Power Sources*, vol. 317, pp. 93–102, 2016.
- [7] M. Winter, G. H. Wrodnigg, J. O. Besenhard, W. Biberacher, and P. Novák, "Dilatometric Investigations of Graphite Electrodes in Nonaqueous Lithium Battery Electrolytes," *J. Electrochem. Soc.*, vol. 147, no. 7, p. 2427, 2000.
- [8] M. N. Obrovac and L. Christensen, "Structural Changes in Silicon Anodes during Lithium Insertion/Extraction," *Electrochem. Solid-State Lett.*, vol. 7, no. 5, pp. A93–A96, 2004.
- [9] J. Cannarella and C. B. Arnold, "Stress evolution and capacity fade in constrained lithium-ion pouch cells," *J. Power Sources*, vol. 245, pp. 745–751, 2014.